Fast Scintillators for High Energy Physics and PET Applications

Snowmass Mu2e-II session

~~KNI/MDL Seminar~~
~~February 4, 2013~~

David Hitlin
Caltech

Fast Scintillators for High Energy Physics and PET Applications

- The thrust in modern HEP experiments is towards the study of ever more elusive processes, at both the Energy Frontier (*e.g.* searching for evidence of supersymmetry at the LHC) and the Intensity Frontier (searching for rare quark and lepton decays). Some examples:
- Muons: $\mu^- \rightarrow e^-$ conversion, $\mu^+ \rightarrow e^+e^+e^-$, $\mu^+ \rightarrow e^+\gamma$, $\mu^+e^- \rightarrow e^+\mu^-$
- Kaons $K^+ \rightarrow \pi^+\nu\bar{\nu}$, $K_L^0 \rightarrow \pi^0\nu\bar{\nu}$
  - Expected rates for these processes are in the range ~10^{-11} to 10^{-18}
  - Requires muon or kaon rates in the range 10^{10} to 10^{11}/second
- Detecting these processes requires efficient detection and reconstruction of the sought-after final state, together with the ability to reject backgrounds, that is events of more common origin that have been mis-measured
- For each candidate rare event, we must measure the charged particle momentum and species, and the energy of photons
  - Efficiency, energy resolution, spatial resolution, angular resolution, time resolution, rate capability, radiation hardness, cost
  - Energy range is MeV to GeV

Example Power Staging Plan for Project X

Program:	Onset of NOvA operations in 2013	Stage-1: 1 GeV CW Linac driving Booster & Muon, n/edm programs	Stage-2: Upgrade to 3 GeV CW Linac	Stage-3: Project X RDR	Stage-4: Beyond RDR: 8 GeV power upgrade to 4MW
MI neutrinos	470-700 kW**	515-1200 kW**	1200 kW	2450 kW	2450-4000 kW
8 GeV Neutrinos	15 kW + 0-50 kW**	0-42 kW* + 0-90 kW**	0-84 kW*	0-172 kW*	3000 kW
8 GeV Muon program e.g, (g-2), Mu2e-1	20 kW	0-20 kW*	0-20 kW*	0-172 kW*	1000 kW
1-3 GeV Muon program, e.g. Mu2e-2	~8 kW	80 kW	1000 kW	1000 kW	1000 kW
Kaon Program	0-30 kW** (<30% df from MI)	0-75 kW** (<45% df from MI)	1100 kW	1870 kW	1870 kW
Nuclear edm ISOL program	none	0-900 kW	0-900 kW	0-1000 kW	0-1000 kW
Ultra-cold neutron program	none	0-900 kW	0-900 kW	0-1000 kW	0-1000 kW
Nuclear technology applications	none	0-900 kW	0-900 kW	0-1000 kW	0-1000 kW
# Programs:	4	8	8	8	8
Total max power:	735 kW	2222 kW	4284 kW	6492 kW	11870kW

$\mu^+ \to e^+\gamma$ MEG and beyond

MEG: $B(\mu^+ \to e^+\gamma) <$ 2.4 x10^{-12} @ 90% CL

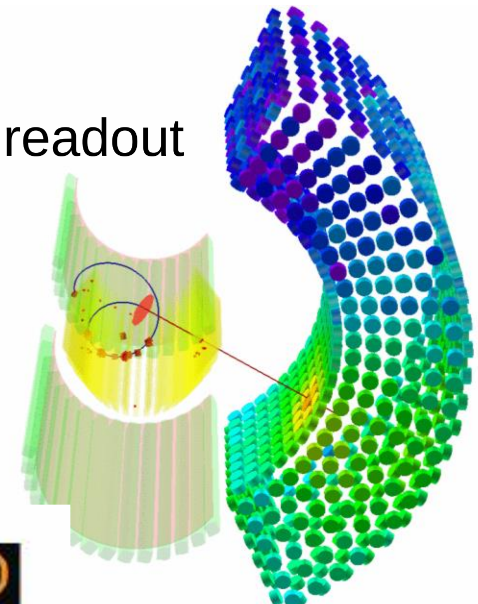

- Uses a LXe calorimeter with (UV sensitive) PMT readout
- Proposed upgrade to sensitivity of 5×10^{-14}
- Calorimeter upgrade: smaller photosensors on entrance face
  - Improve shower localization and, thereby, time resolution, to improve sensitivity

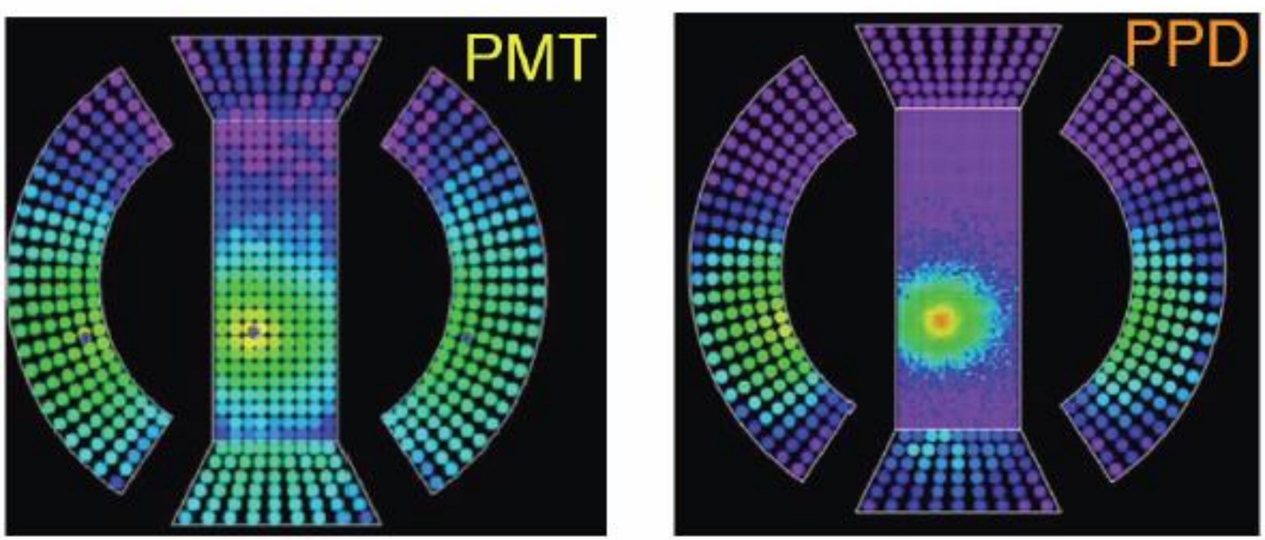

Mu2e Search for $\mu^- \to e^-$ conversion at 6x10^{-17}

Production Solenoid

- Production target
- Graded field

- Delivers ~ 0.0016 stopped μ^- per incident proton
- 10^{10} Hz of stopped muons

Detector Solenoid

- Muon stopping target
- Tracker
- Calorimeter
- Warm bore evacuated to 10^{-4} Torr

Transport Solenoid

- Collimation system selects muon charge and momentum range
- Pbar window in middle of central collimator

Cosmic Ray Veto not shown

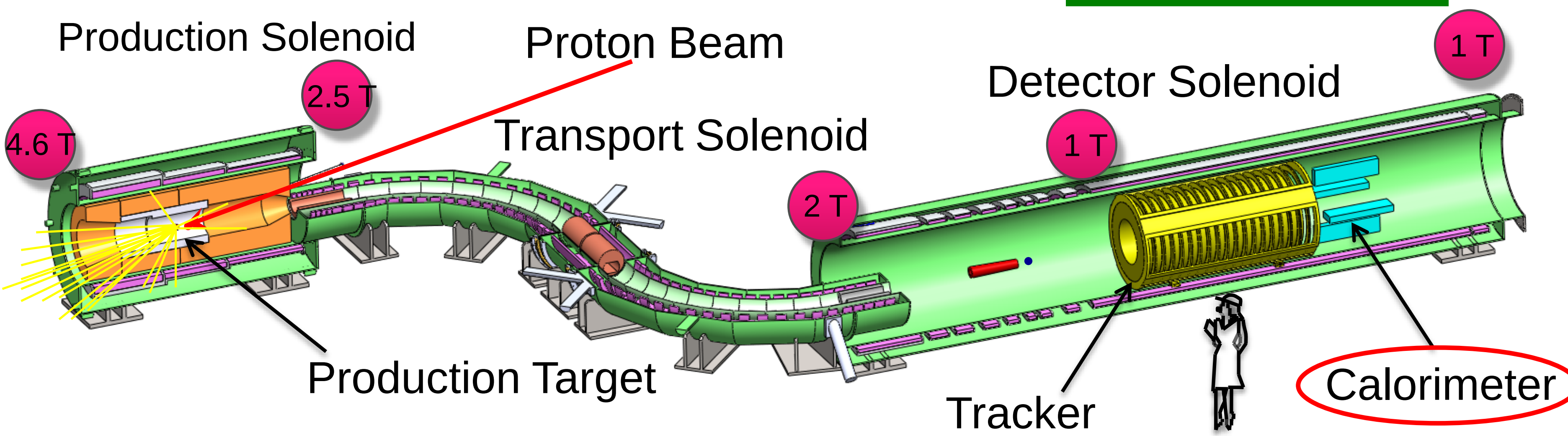

Mu2e calorimeter requirements

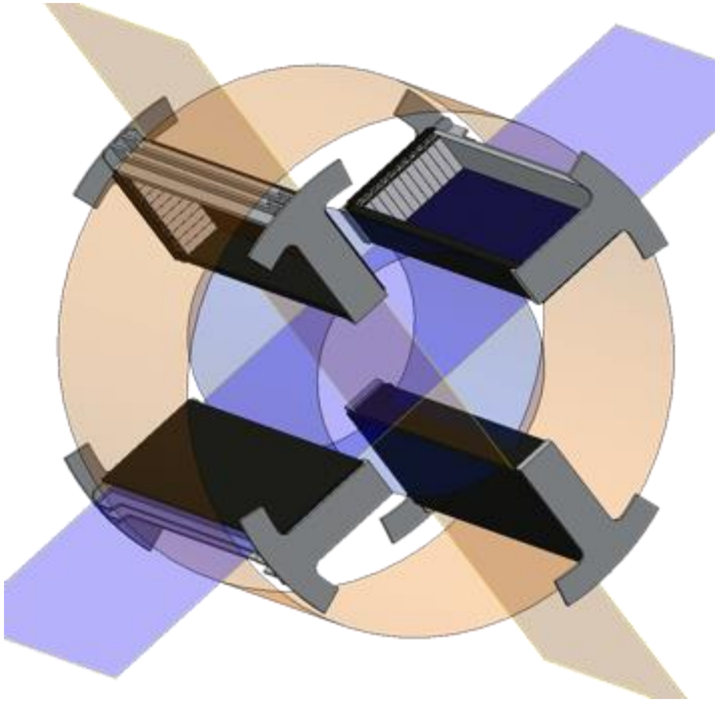

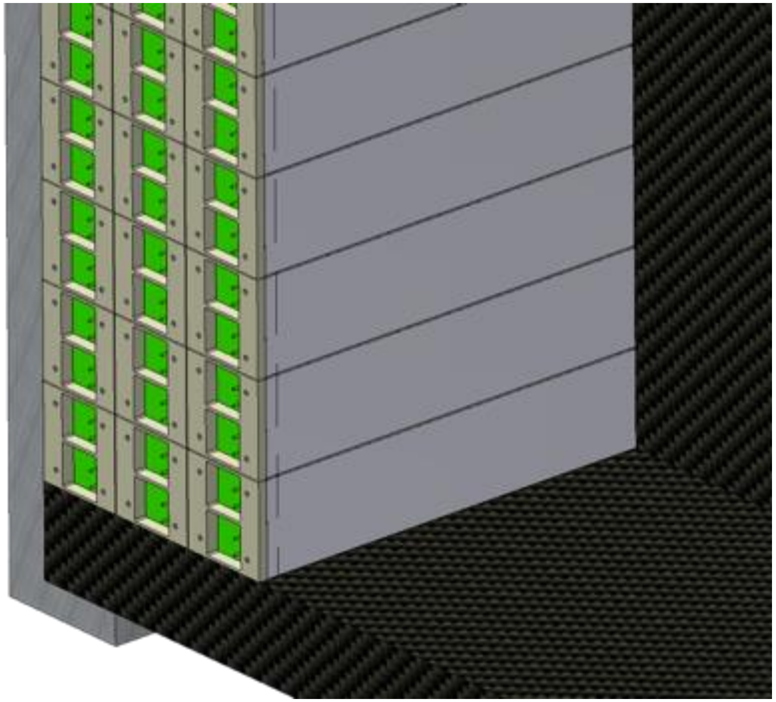

Requirements are met by an array of ~2100 LYSO crystals (11 X_0)

Mu2e calorimeter requirements

The purpose of the calorimeter is to confirm that a reconstructed track of a $\mu \to e$ conversion electron candidate is well-measured, and was not created by a spurious combination of hits in the tracker.

1. Measure the position of the conversion electron $\to \sigma(x) \leq \mathcal{O}$ (1 cm).
2. Compare the energy deposited in the calorimeter to the reconstructed track momentum $\to \sigma(E) \leq \mathcal{O}$ (2%), with an uncertainty in the energy scale small compared to the resolution.
3. Compare the time of the energy deposit in the calorimeter to the time determined from the tracker $\to \sigma(t)\ \mathcal{O}$ (≤1 ns).
4. Provide particle identification to separate, for example, electrons from muons
5. Provide a trigger that can be used for event selection
6. Maintain functionality in a 50 Gy/year radiation environment with light yield loss < 10%

Requirements are met by an array of ~2100 LYSO crystals (11 X_0)

Effect of background on conversion electron resolution

- "Salt and pepper" background included in energy clusters
  - Deteriorates energy resolution

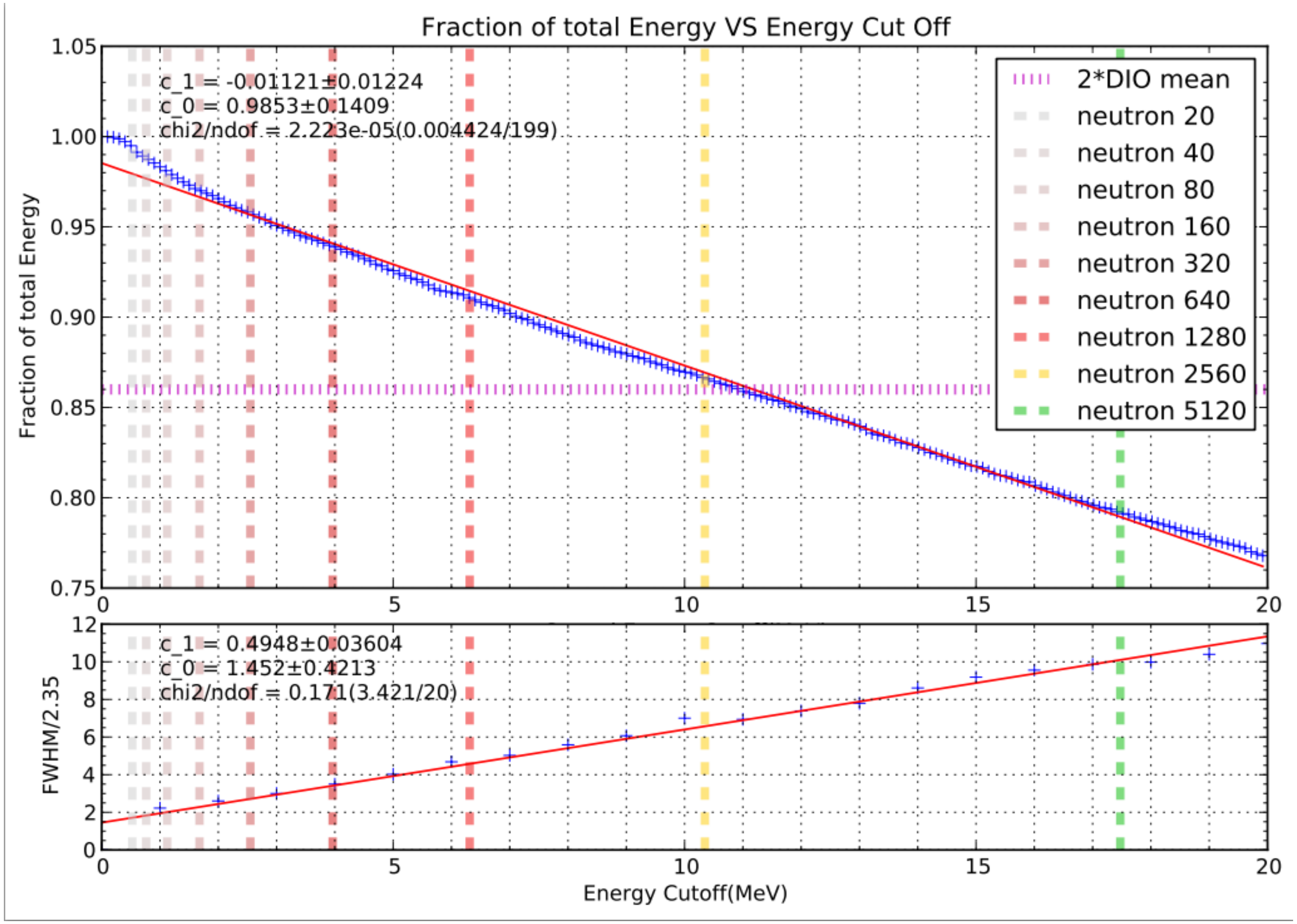

At PX Stage 1, requirements can likely be ~met by shortening integration time.

Tracker ??????

At later stages, either a new technique or a faster crystal will be needed

PET scanning is another area utilizing crystal scintillators

- Utilize biologically active radioactive positron emitters, such as ^{11}C, ^{13}N, ^{15}O, ^{18}F, ^{82}Rb
- Detect 0.511 MeV gammas from positron annihilation using scintillating crystals, such as LYSO or BGO
- Faster scintillators would be an advantage in reducing dose rates and improving resolution via transit time measurements

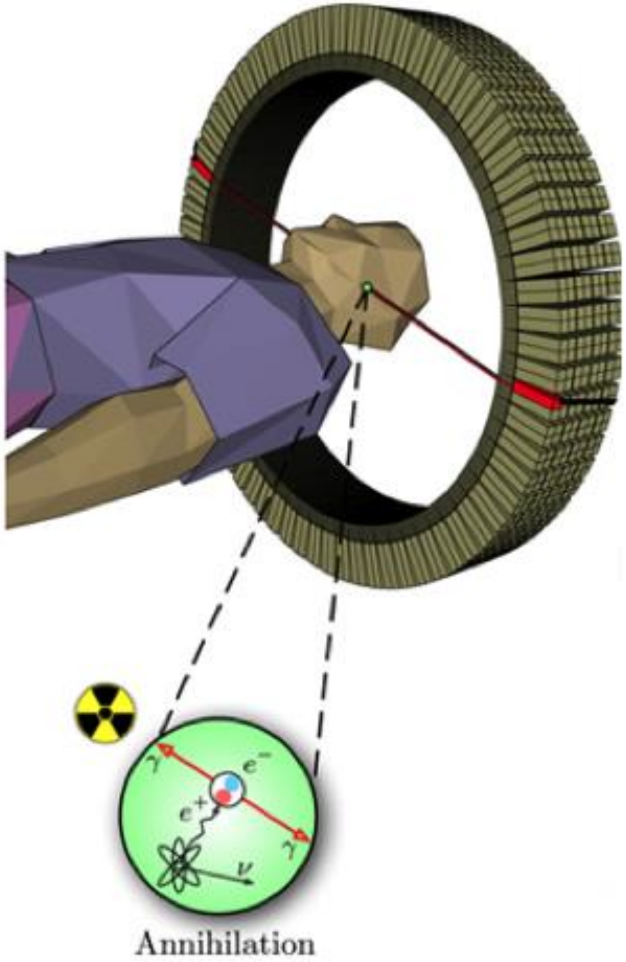

PET scanning

- Time resolution provides an independent spatial measurement
  - Can reduce the scan time, and thus the dose rate to achieve a given spatial resolution

No timing   With timing

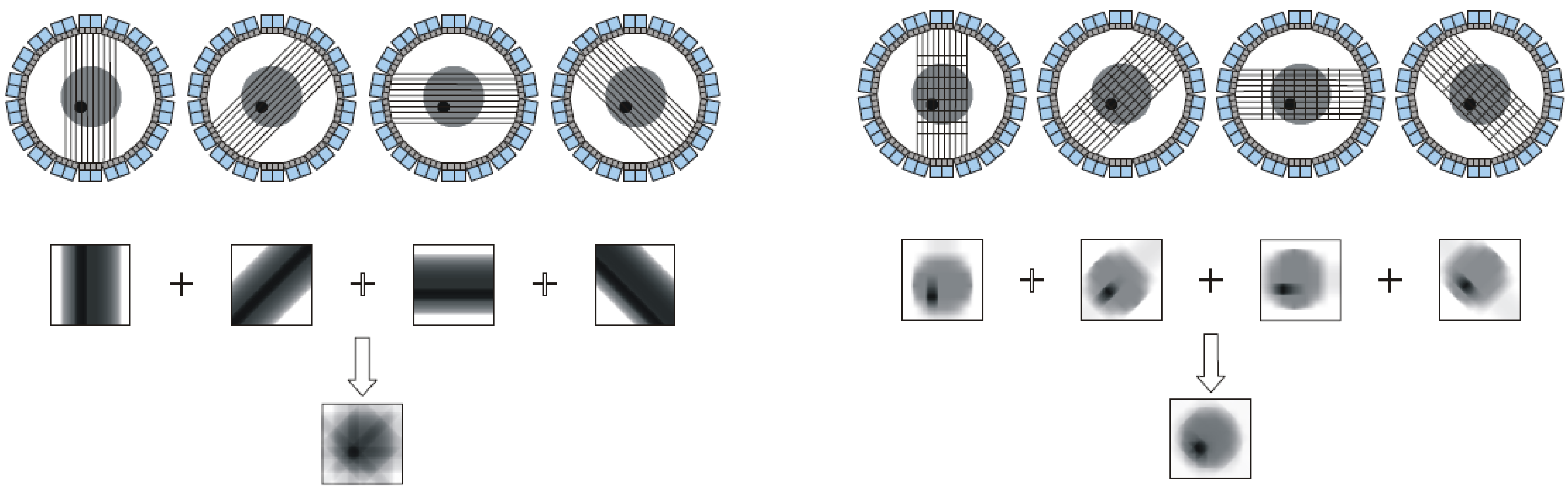

A time resolution of 50ps yields a spatial resolution of ~8mm

Can improve resolution with new scintillators

Hardware	Δt (ps)	TOF Gain
BGO Block Detector	3000	0.8
LSO Block (non-TOF)	1400	1.7
LSO Block (TOF)	550	4.2
$LaBr_3$ Block	350	6.7
LSO Single Crystal	210	11.1
LuI_3 Single Crystal	125	18.7
$LaBr_3$ Single Crystal	70	33.3

Research $LaBr_3$ Camera Built by U. Penn
~350 ps Intrinsic Detector Resolution
420–500 ps Camera Resolution (Electronics Limited)

Fast scintillating crystals

	LSO/LYSO	YSO	GSO	BaF_2	CsI	CeF_3	$CeBr_3$	$LaBr_3$	$LaCl_3$
Density (g/cm^3)	7.40	4.54	6.71	4.89	4.51	6.16	5.10	5.29	3.86
Radiation Length (cm)	1.14	3.04	1.38	2.03	1.86	1.70	1.96	1.88	2.81
Molière Radius (cm)	2.07	2.87	2.23	3.10	3.57	2.41	2.97	2.85	3.71
Interaction Length (cm)	20.9	27.3	22.2	30.7	39.3	23.2	31.5	30.4	37.6
Z value	64.8	33.3	57.9	51.6	54.0	50.8	45.6	45.6	47.3
dE/dX (MeV/cm)	9.55	6.70	8.88	6.52	5.56	8.42	6.65	6.90	5.27
Emission Peak[a] (nm)	420	420	430	300 220	420 310	340 300	371	356	335
Refractive Index[b]	1.82	1.80	1.85	1.50	1.95	1.62	2.3	1.9	1.9
Relative Light Yield[a,c]	100	40		42 4.8	4.2 1.3	8.6	144	153	15 49
Decay Time[a] (ns)	40	70	65	650 0.9	30 6	30	17	20	570 24
d(LY)/dT [d] (%/°C)	-0.2	-0.3	-0.7	-1.9 0.1	-1.4	~0	-0.1	0.2	0.1

Ren-yuan Zhu

Scintillation pulse shapes

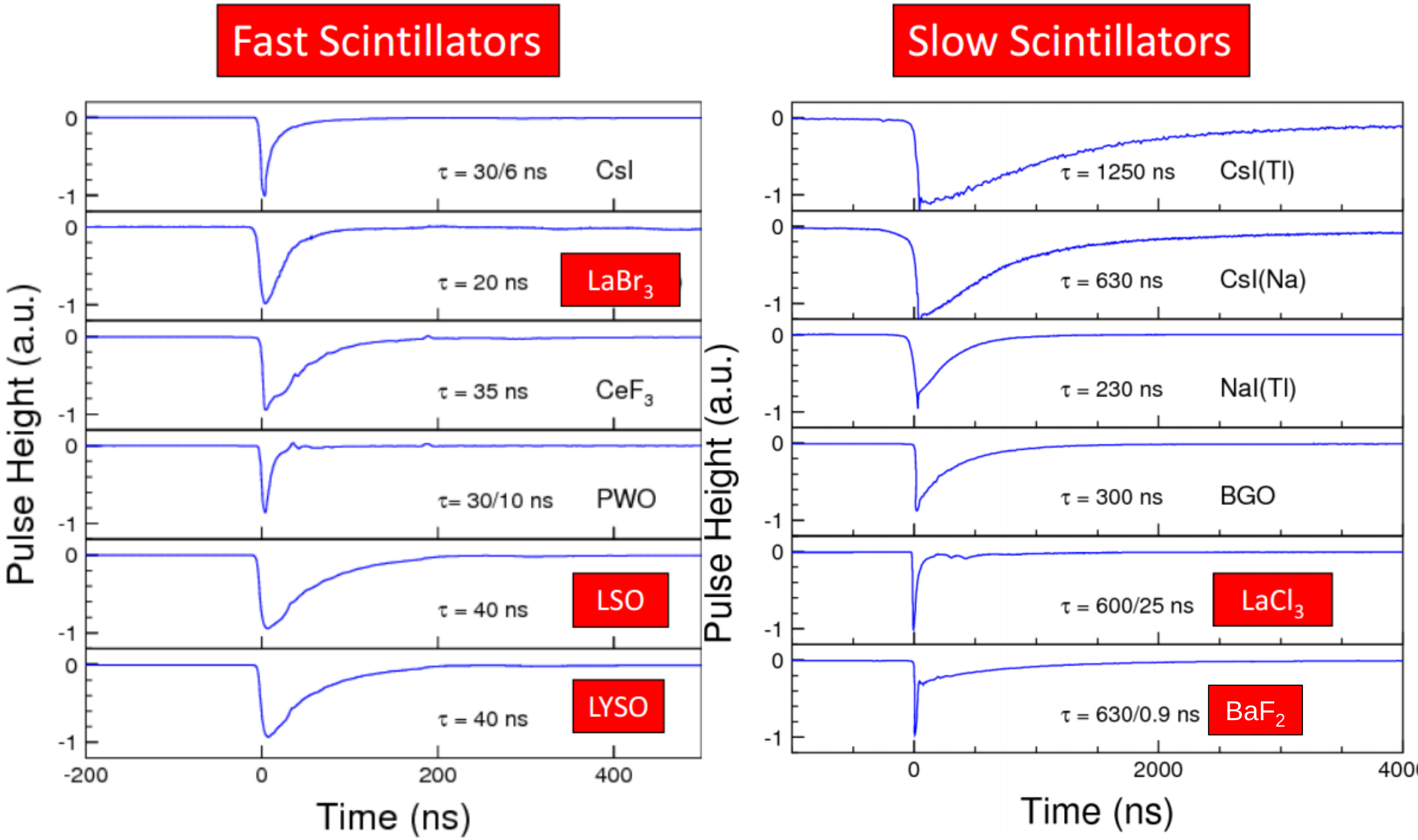

Ren-yuan Zhu

Rise and decay times matter, as does crystal size

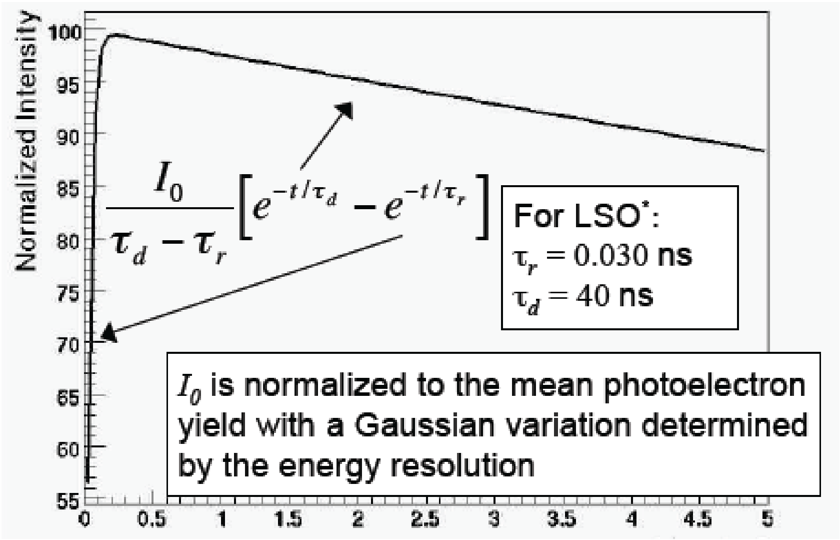

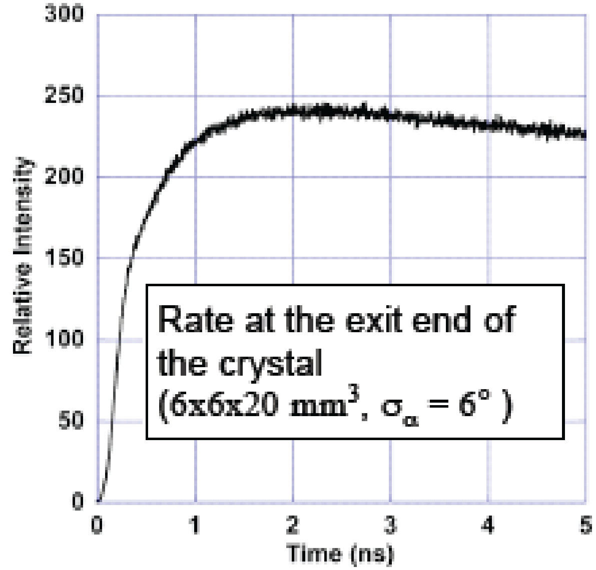

$$\mathrm{var}(t) \approx \frac{\bar{t}^2}{N}\left[1 + \frac{N+1}{I_0} + \ldots\right]$$

where

$$\bar{t} \approx \frac{N\tau_d}{I_0}\left[1 + \frac{N+1}{2I_0} + \ldots\right]$$

A fast crystal “figure of merit”

Crystal Scintillators	Relative LY (%)	A_1 (%)	τ_1 (ns)	A_2 (%)	τ_2 (ns)	Total LO (p.e./MeV, XP2254B)	LO in 1ns (p.e./MeV, XP2254B)	LO in 0.1ns (p.e./MeV, XP2254B)	LY in 0.1ns (photons/MeV)
BaF_2	40.1	91	650	9	0.9	1149	71.0	11.0	136.6
LSO:Ca,Ce	94	100	30			2400	78.7	8.0	110.9
LSO/LYSO:Ce	85	100	40			2180	53.8	5.4	75.3
CeF_3	7.3	100	30			208	6.8	0.7	8.6
BGO	21	100	300			350	1.2	0.1	2.5
PWO	0.377	80	30	20	10	9.2	0.42	0.04	0.4
$LaBr_3$:Ce	130	100	20			3810	185.8	19.0	229.9
$LaCl_3$:Ce	55	24	570	76	24	1570	49.36	5.03	62.5
NaI:Tl	100	100	245			2604	10.6	1.1	14.5
CsI	4.7	77	30	23	6	131	7.9	0.8	10.6
CsI:Tl	165	100	1220			2093	1.7	0.2	4.8
CsI:Na	88	100	690			2274	3.3	0.3	4.5

Motivates R&D on fast crystals and appropriate solid state readout

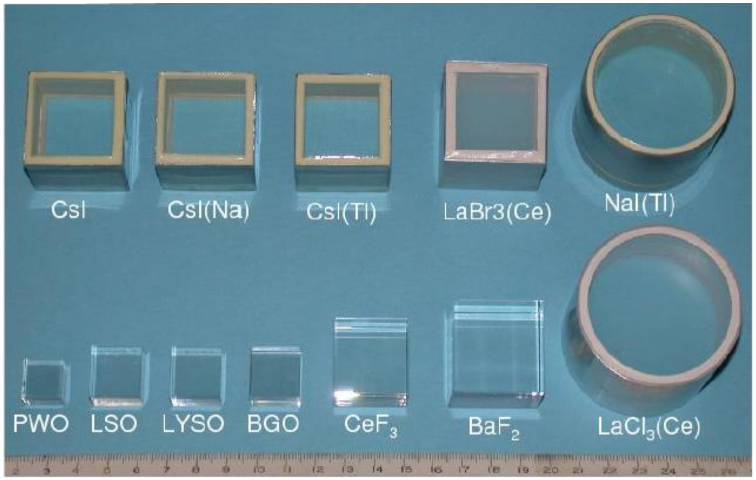

Ren-yuan Zhu

BaF_2 is a potentially attractive high rate crystal

- BaF_2 is among the fastest scintillating crystals (0.9ns), but there is a much larger, slower, component (650ns)

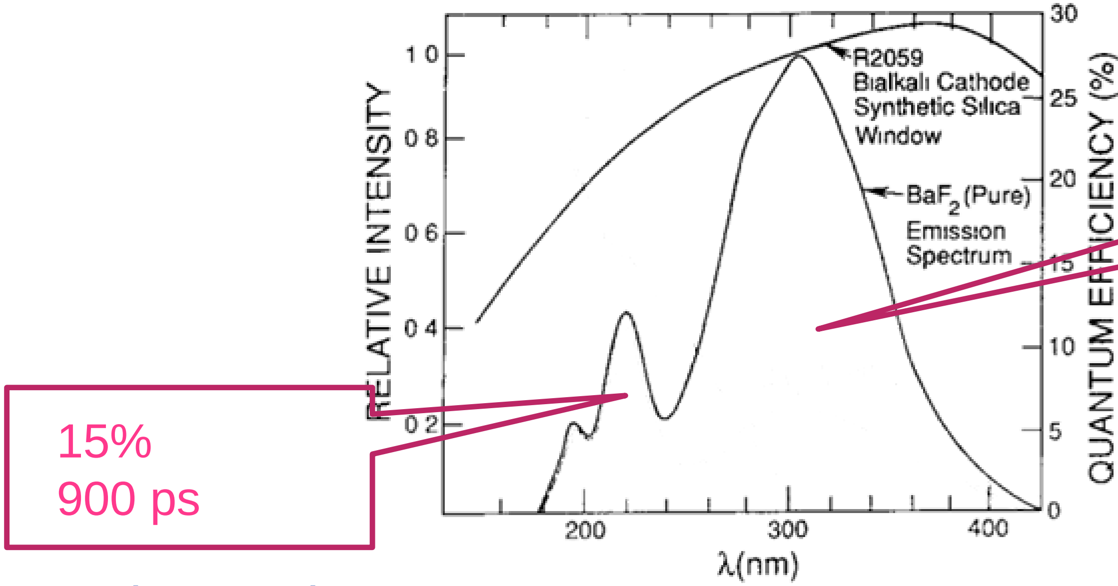

Total light output
1.2×10^4 photons/MeV

- In order to take advantage of the fast component, it is necessary to suppress the slow component

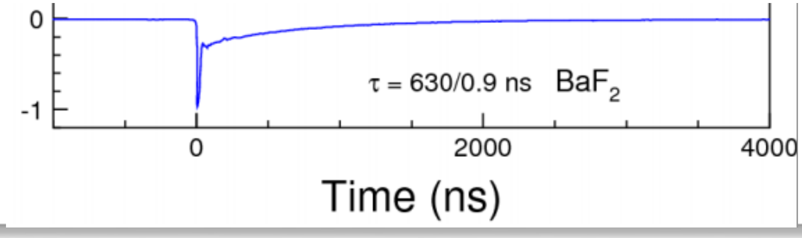

BaF_2 is a potentially attractive high rate crystal

- BaF_2 is among the fastest scintillating crystals (0.9ns), but there is a much larger, slower, component (650ns)

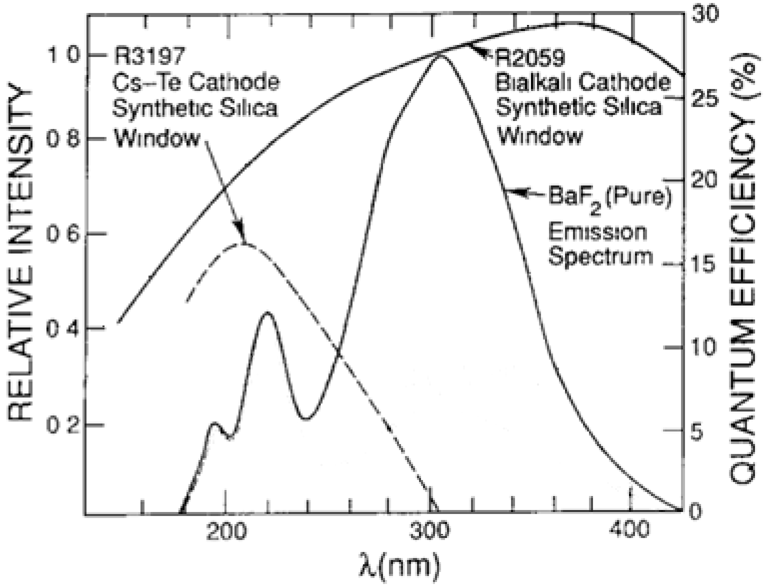

Can solar blind SiC APDs, which now exist at 100 μm diameter, be made larger, and combined with a thin film optical filter, to make BaF_2 a truly fast scintillator?

- In order to take advantage of the fast component, it is necessary to suppress the slow component:
  - Need a "solar-blind" photosensor

BaF_2 is a potentially attractive high rate crystal

- BaF_2 is among the fastest scintillating crystals (0.9ns), but there is a much larger, slower, component (650ns)

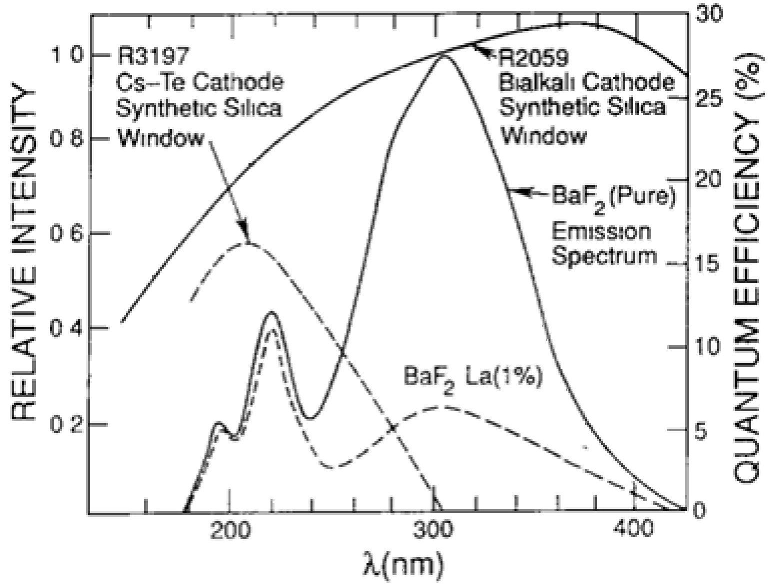

- In order to take advantage of the fast component, it is necessary to suppress the slow component
  - La doping of pure BaF2 suppresses slow component by ~4

Solar-blind photosensors

- Solar-blind PMTs exist
  - Large area, fast, but expensive, and do not work in a magnetic field
- Solar-blind solid state devices also exist
  - SiC APDs (100μm diameter)
  - AlGaN APDs (< 1mm diameter)
- There are several potential approaches to fast, large area, solar-blind, magnetic field insensitive photosensors
  - A variant of the LAPPD channel plate
  - SiPMs with antireflection coatings
  - Large area back-illuminated delta-doped APDs

Back-illuminated delta-doped sensors

- The JPL microelectronics group (M. Hoenk, *et al*.) has developed a technique to produce CCD imaging devices with excellent sensitivity in the UV
  - These have been used, for example, on the Cassini mission
  - The process starts with existing CCD chips in wafer form, thinned (to 10-15μm). They believe that the technique will work with APDs.
  - Using molecular beam epitaxy, a monolayer of boron is deposited to create a potential well n

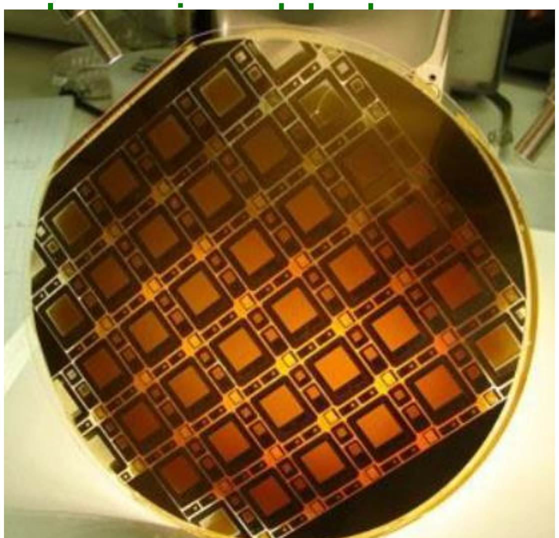

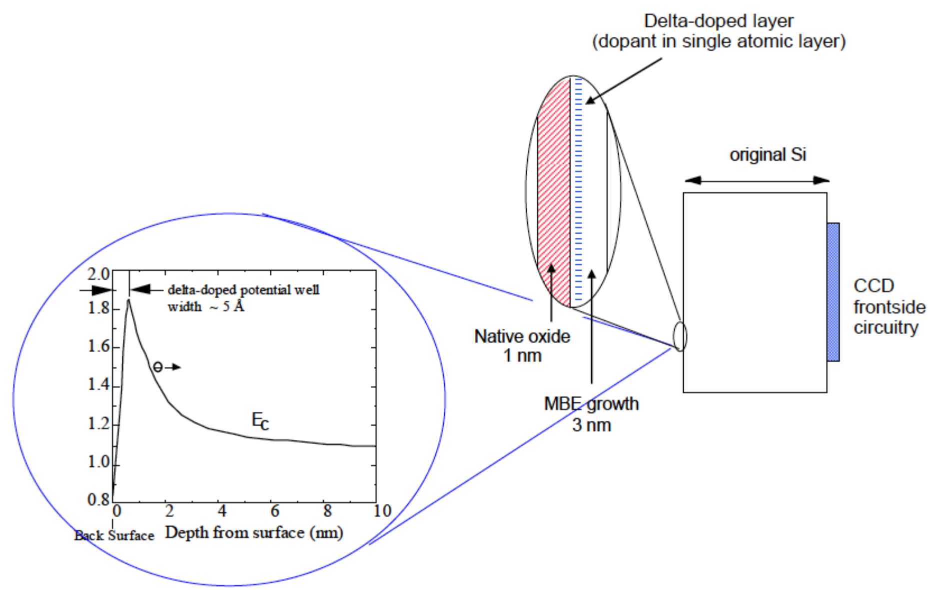

National Aeronautics and Space Administration

Visible-blind, Superlattice-doped Silicon Detectors: Structure, Fabrication and Physics

Michael Hoenk
Microdevices Laboratory (MDL)
Jet Propulsion Laboratory
California Institute of Technology

Presentation to Kavli Nanoscience Institute
February 4, 2013

The work described here was carried out by the Jet Propulsion Laboratory, California Institute of Technology, under a contract with the National Aeronautics and Space Administration.

JPL / Caltech Collaborations

- Professor David Hitlin
  - Experimental High Energy Physics
  - Visible-blind APDS for ultrafast scintillators
- Professor Chris Martin
  - PI of GALEX
  - Photon counting ultraviolet spectroscopy detectors for UV astrophysics
- Professor Shri Kulkarni
  - Director, Caltech Optical Observatories
  - UV imaging detectors for transient astronomy

Part 1: Structure of silicon avalanche photodiodes

…and the importance of atomic scale interface engineering

Reach-Through Avalanche Photodiode (RTAPD)

Reverse biased photodiode with $p^{+}\pi p n^{+}$ structure

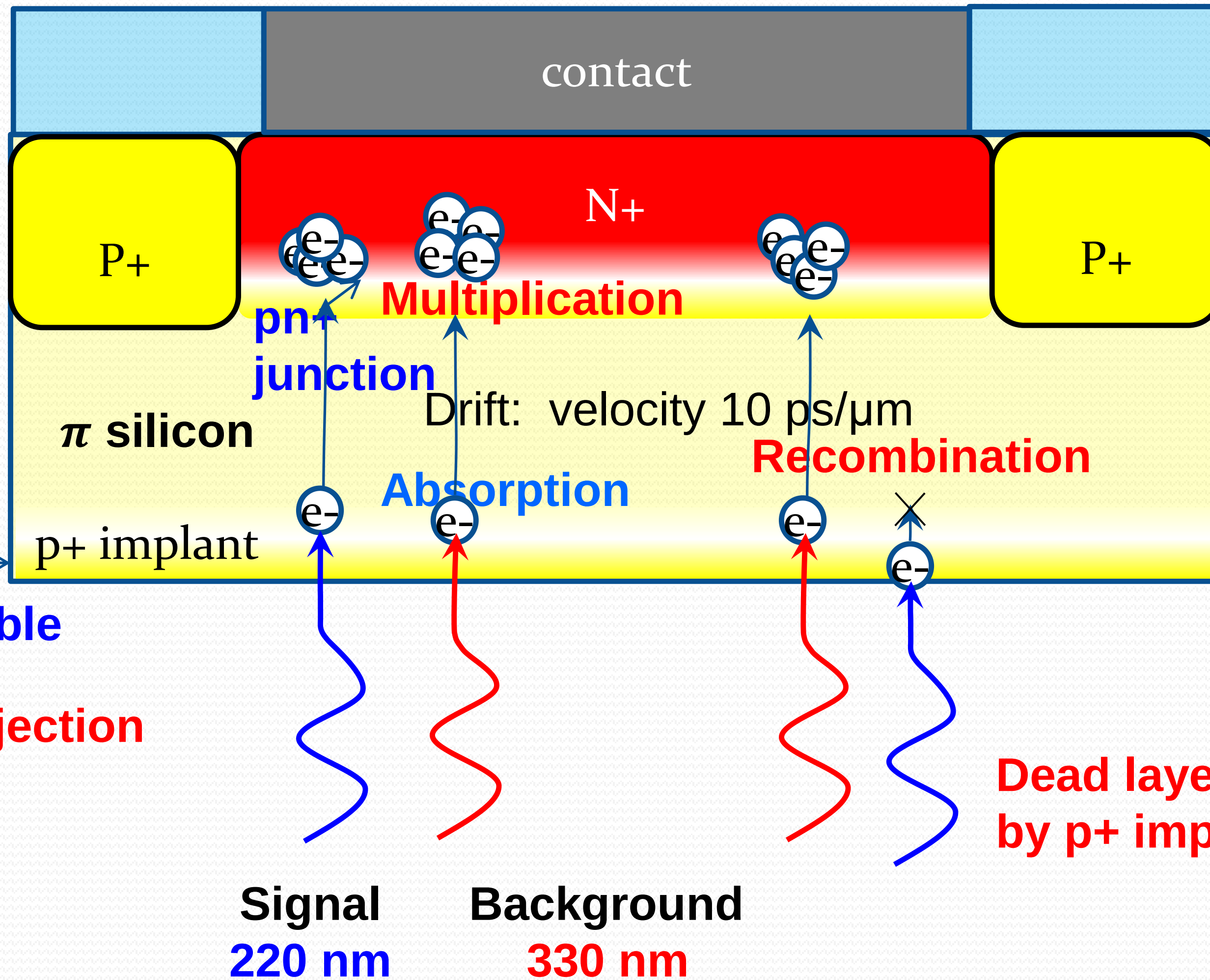

Avalanche gain in pn+ junction

Electric field drives electrons toward junction

Deep implant

UV QE Low, unstable

No background rejection

Dead layer formed by p+ implant

Ultraviolet light is absorbed near the surface

Delta doping for Surface Passivation

Self-ordered surface phase:
Boron on Silicon <100>

- 2D doping → Delta-doping
- Dopant density as high as $10^{22}cm^{-3}$

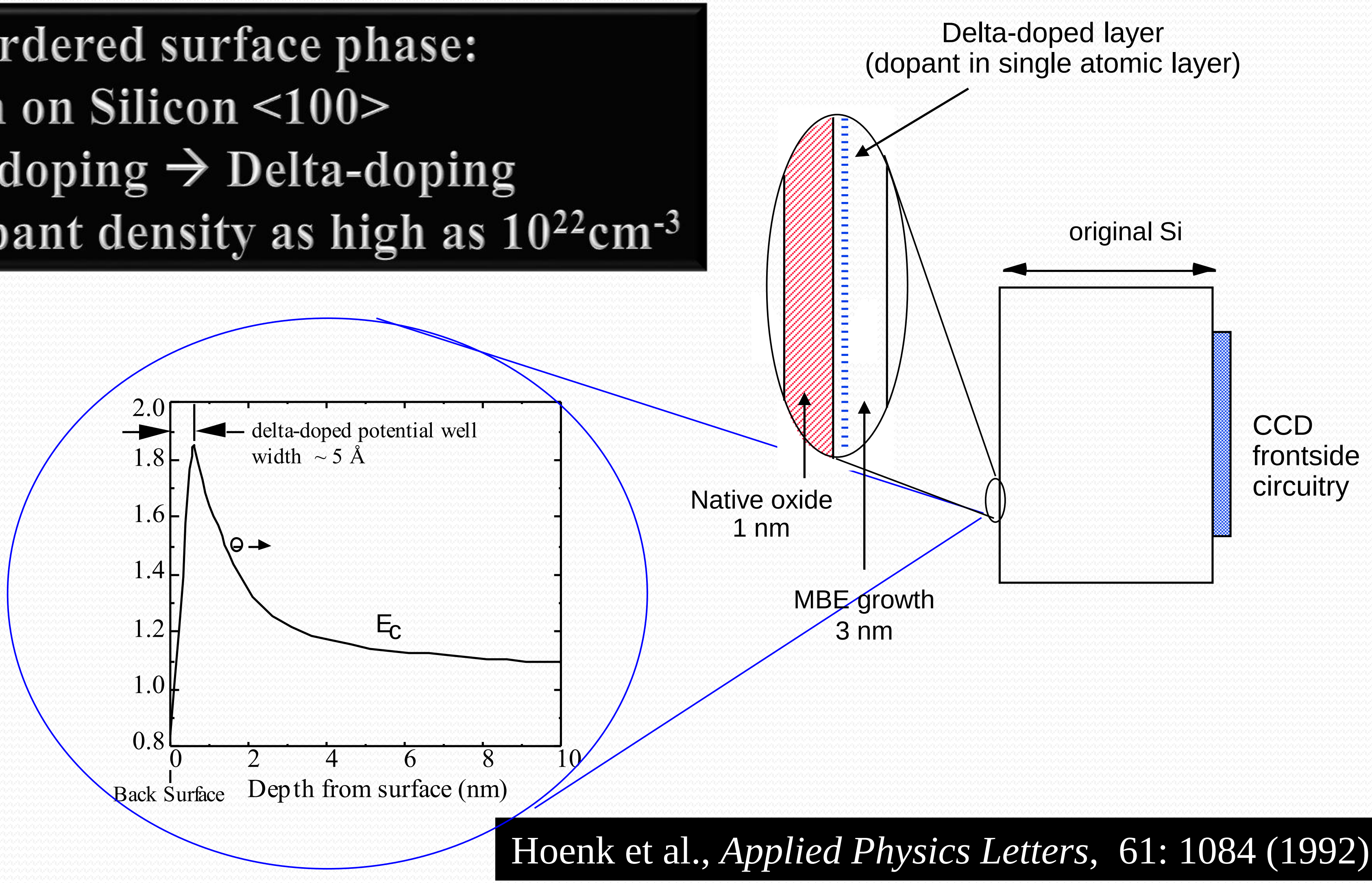

Hoenk et al., *Applied Physics Letters*, 61: 1084 (1992)

Fully-processed devices are modified using Molecular Beam Epitaxy (MBE)

Photometric stability of Delta-doped detectors

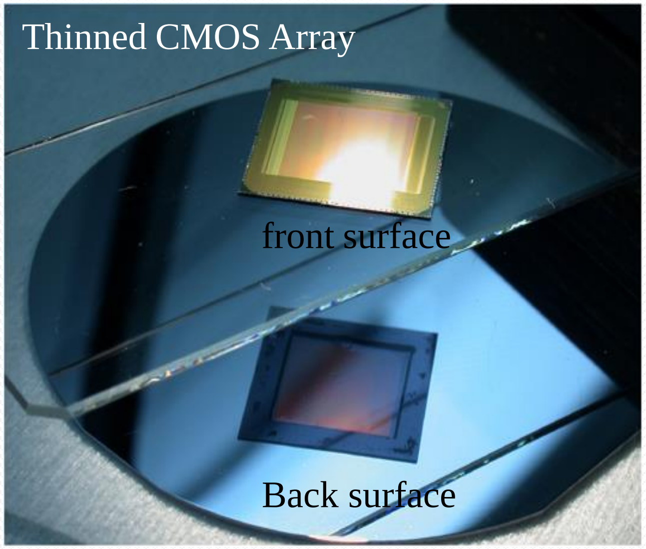

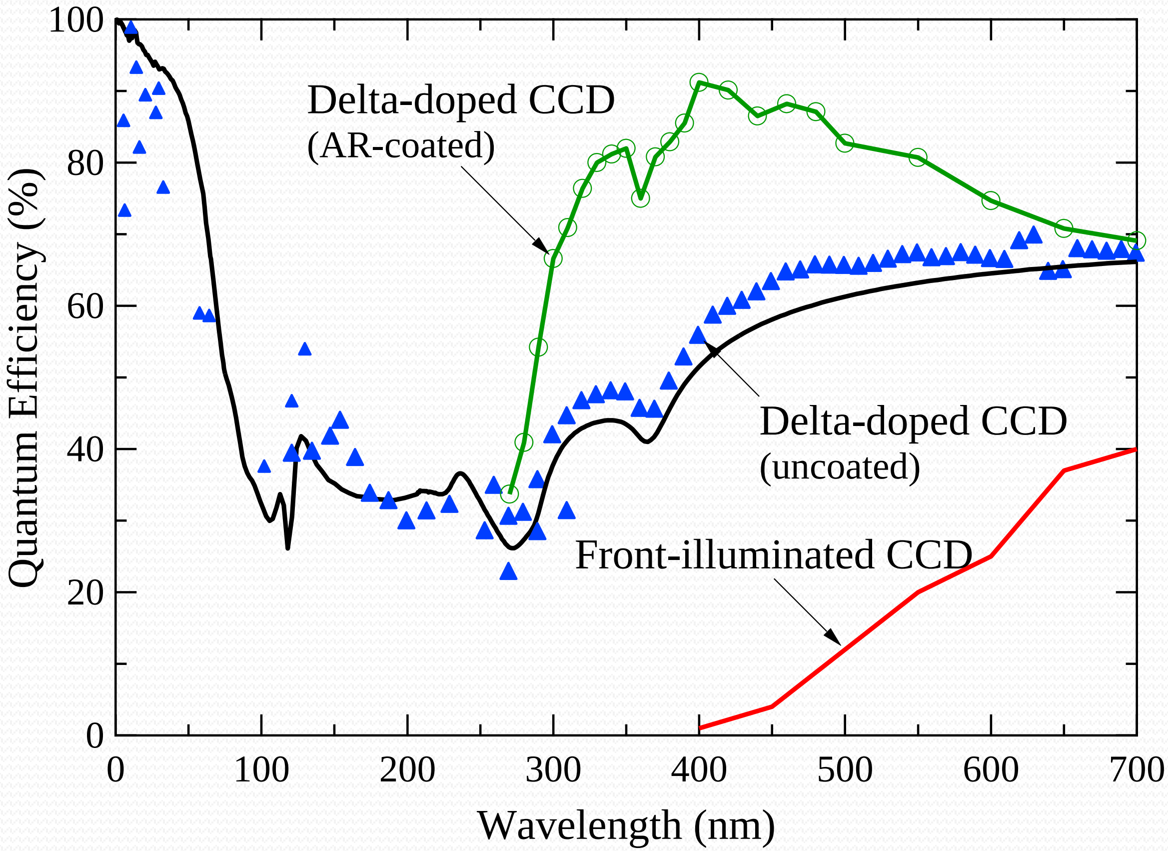

S. Nikzad, "Ultrastable and uniform EUV and UV detectors," *SPIE Proc.*, Vol. 4139, pp. 250-258 (2000).

J. Trauger (PI WF/PC2) – *No measurable hysteresis in delta-doped CCDs*

Atomic Layer Deposition (ALD)

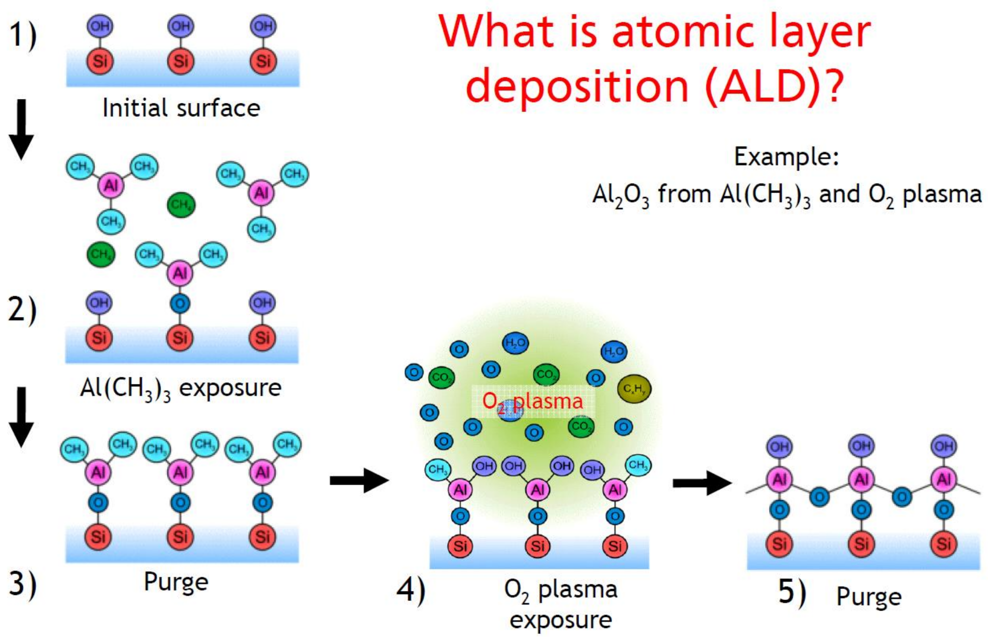

Atomic Layer Deposition is a ***uniquely enabling*** surface and materials engineering technology

- Achieves Layer by Layer growth of films with ***Angstrom*** level control over arbitrarily large surface areas
- Wide suite of materials metals, oxides, and nitrides with excellent film properties
- Can be directly integrated into existing detectors/instruments to vastly improve performance

TEM images of ultra-thin (3.5nm), conformal ALD film

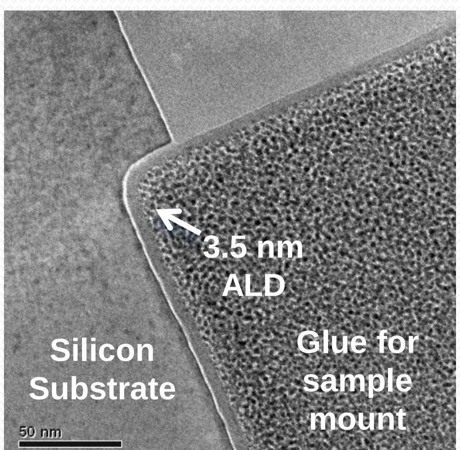

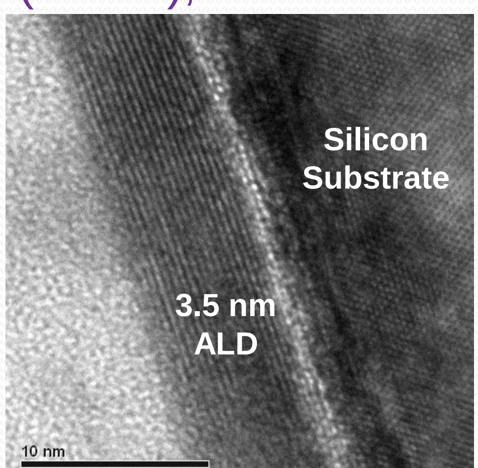

Key Advantages of ALD

- Fully complements the surface engineering capabilities of Si MBE with atomic control of ALD

- Thickness can be specified with Angstrom resolution
  - -Enables precise, repeatable targeting of bands *e.g.* 16.5nm vs. 23nm of Al_2O_3

- Process is completely independent of device size

Far ultraviolet, Visible-blind coatings

"Ultraviolet antireflection coatings for use in silicon detector design,"
Erika T. Hamden, Frank Greer, Michael E. Hoenk, Jordana Blacksberg, Matthew R. Dickie, Shouleh Nikzad, D. Christopher Martin, and David Schiminovich
Applied Optics, Vol. 50, Issue 21, pp. 4180-4188 (2011)

"Delta-doped electron-multiplied CCD with absolute quantum efficiency over 50% in the near to far ultraviolet range for single photon counting applications"
Shouleh Nikzad, Michael E. Hoenk, Frank Greer, Blake Jacquot, Steve Monacos, Todd J. Jones, Jordana Blacksberg, Erika Hamden, David Schiminovich, Chris Martin, and Patrick Morrissey
Applied Optics, Vol. 51, Issue 3, pp. 365-369 (2012)

"Atomically precise surface engineering of silicon CCDs for enhanced UV quantum efficiency,"
Frank Greer, Erika Hamden, Blake C. Jacquot, Michael E. Hoenk, Todd J. Jones, Matthew R. Dickie, Steve P. Monacos, Shouleh Nikzad
J. Vac. Sci. Technol., A 31, 01A103 (2013)

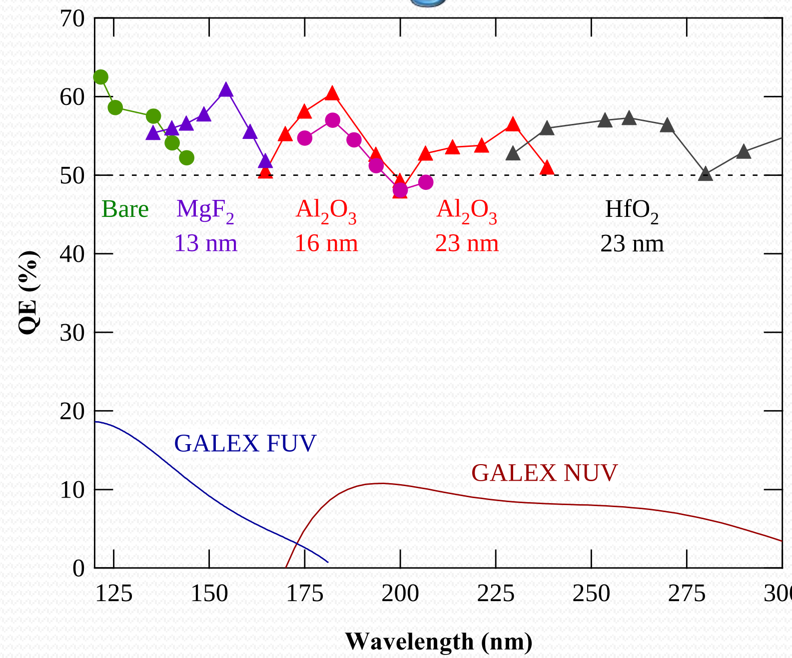

World record deep ultraviolet QE

- **QE > 5x Galex**
- **Stable**
- **Visible blind coatings are possible**

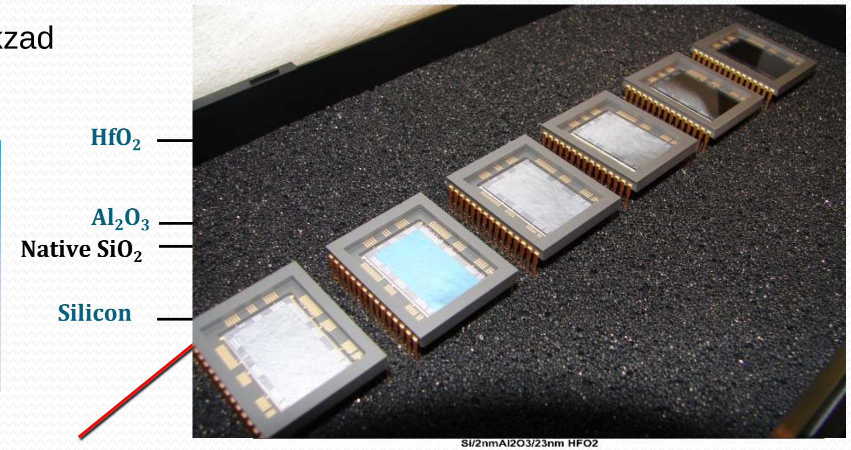

Atomic layer deposition → atomic scale engineering of silicon-dielectric interface

Visible Blocking Designs for 200-235 nm

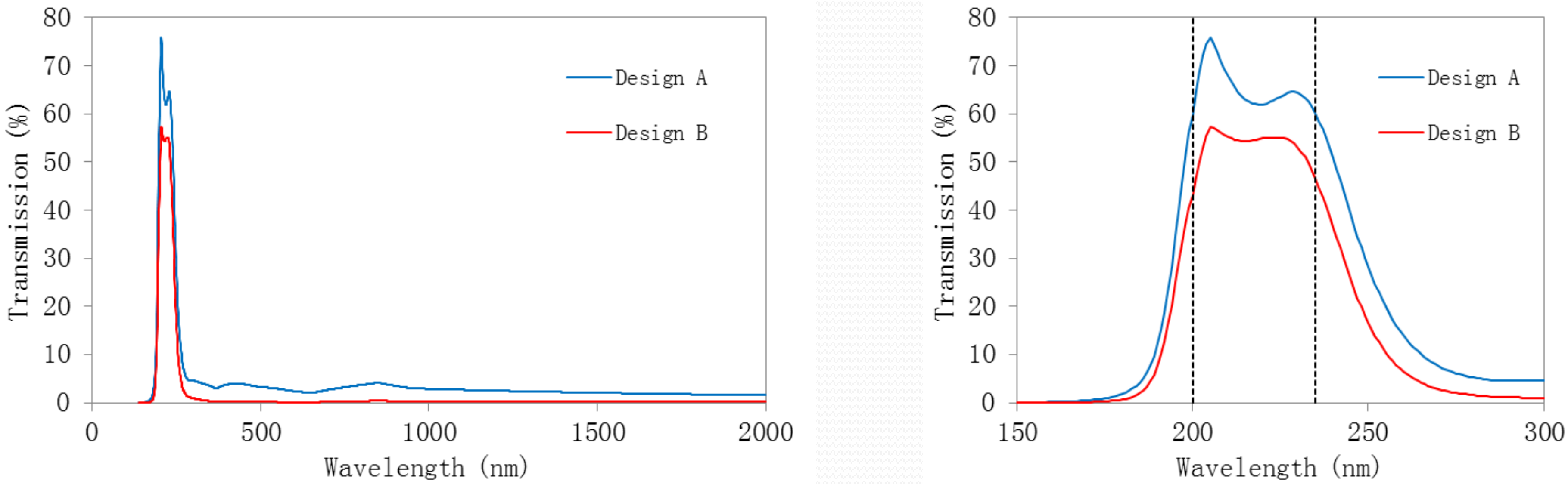

- Initial designs, full design space not completely explored (choice of dielectric, number of layers vs blocking ability etc...)
- Both designs 5 layer stack metallic aluminum and Al_2O_3
  - Design A: 37.8 nm Al_2O_3 / 14.6 nm Al / 33.7 nm Al_2O_3 / 4.7 nm Al / 41.3 nm Al_2O_3
  - Design B: 39.1 nm Al_2O_3 / 18.1 nm Al / 33.2 nm Al_2O_3 / 15.4 nm Al / 17.7 nm Al_2O_3
- Design A: Avg T (200-235 nm) = 65.4%, Avg T (400-1000) = 3.16% → [~21:1]
  - Average transmission in passband can match single layer Al_2O_3
- Design B: Avg T (200-235 nm) = 53.5%, Avg T (400-1000) = 0.23% → [~234:1]
  - Giving up more passband T or narrowing can further improve blocking ratio
- Assumes thin Al layers will behave optically like bulk n,k
  - No stable ALD process exists yet...

Integrated interference filter

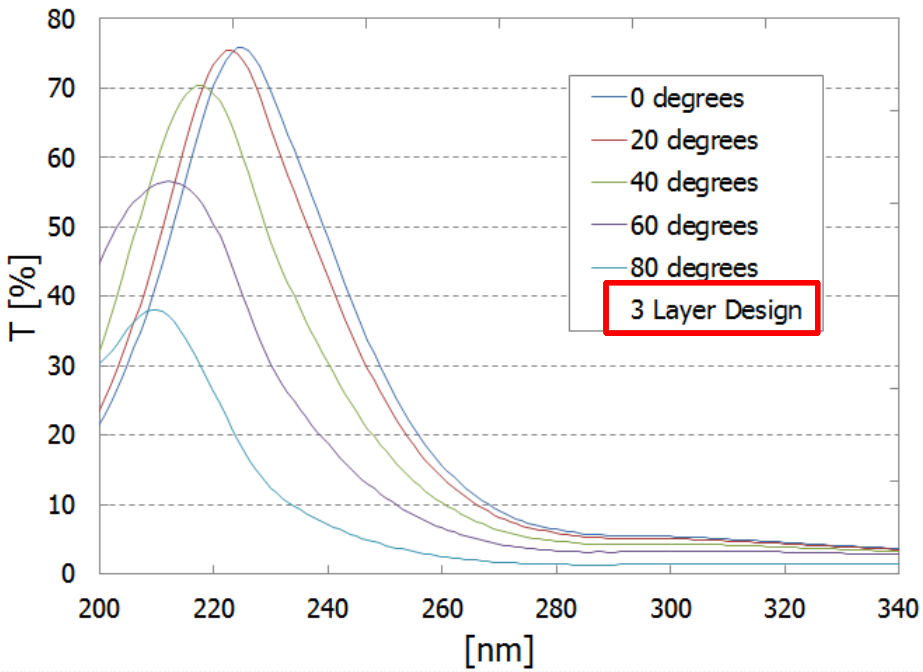

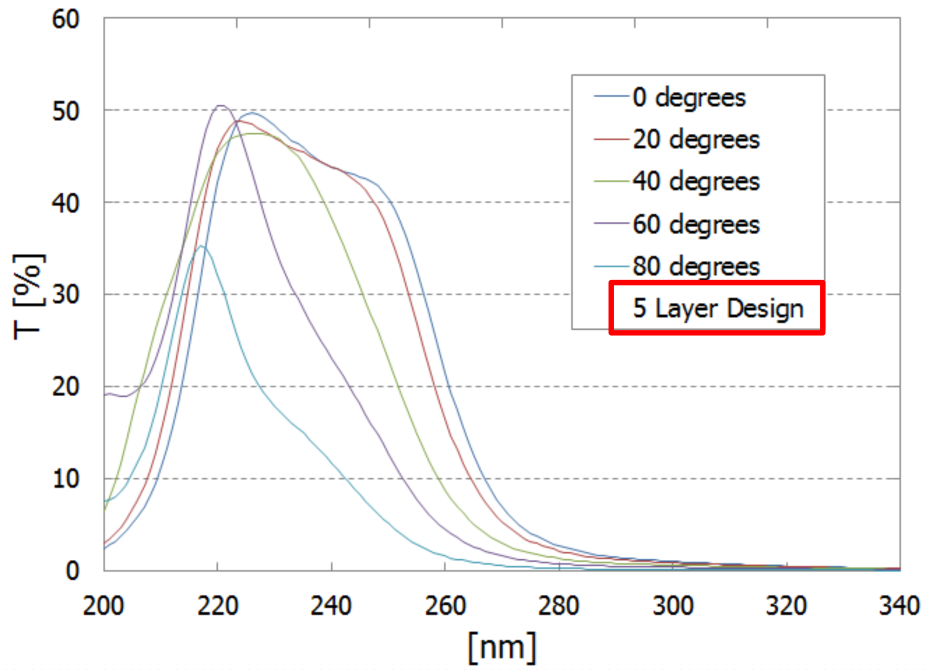

Wafer-scale EMCCD process flow

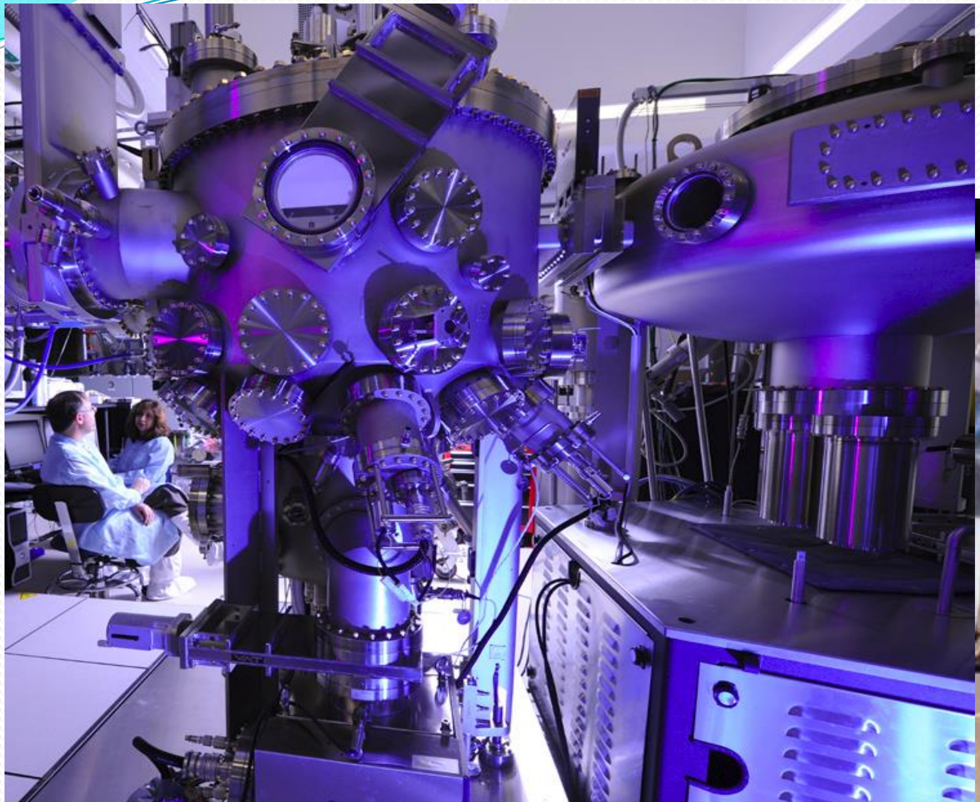

Veeco 8-inch Silicon MBE at JPL's Microdevices Lab

Process steps…

- Wafer-wafer bonding
- Thinning
- MBE growth
- ALD coating
- Patterning
- Etching
- Dicing
- Packaging

Wafer with CMOS imaging arrays

Electron-Multiplying CCD

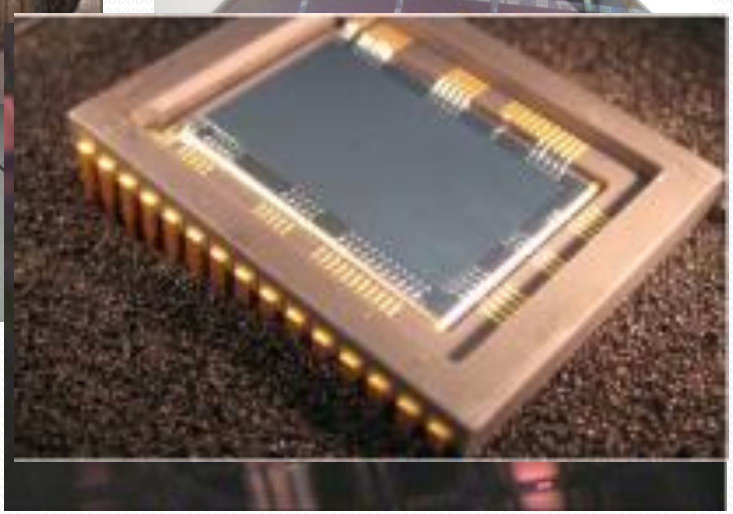

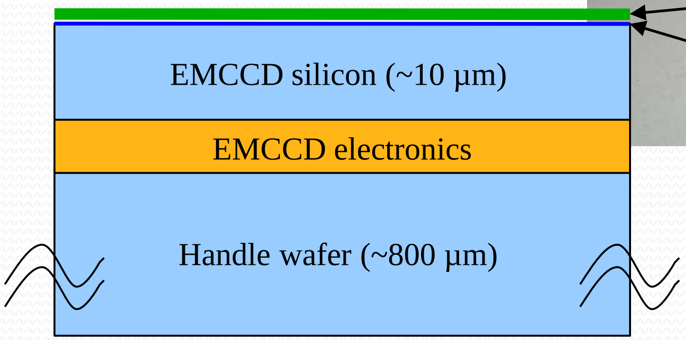

Delta-doping and Quantum Exclusion

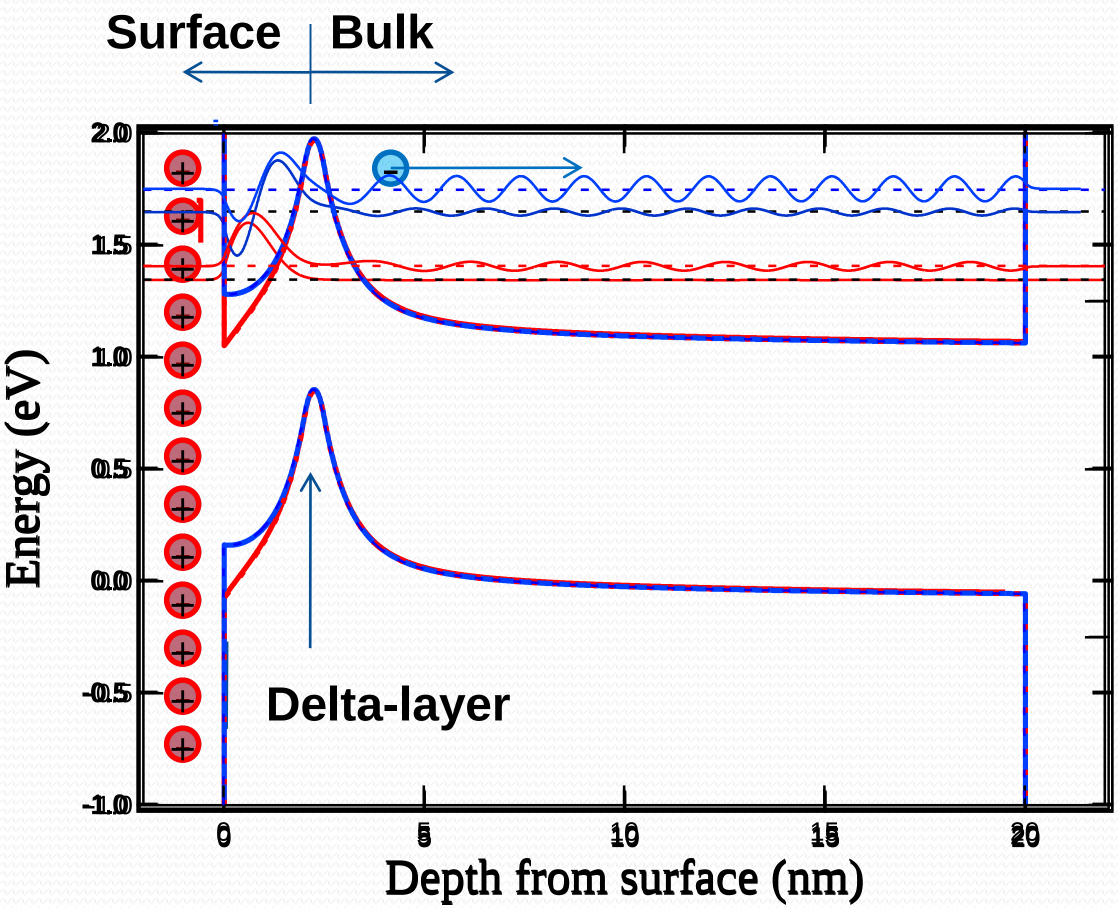

Quantum Exclusion → Elimination of trapping

Positively charged surface @ 10^{13} cm^{-2}

Delta-doped surface

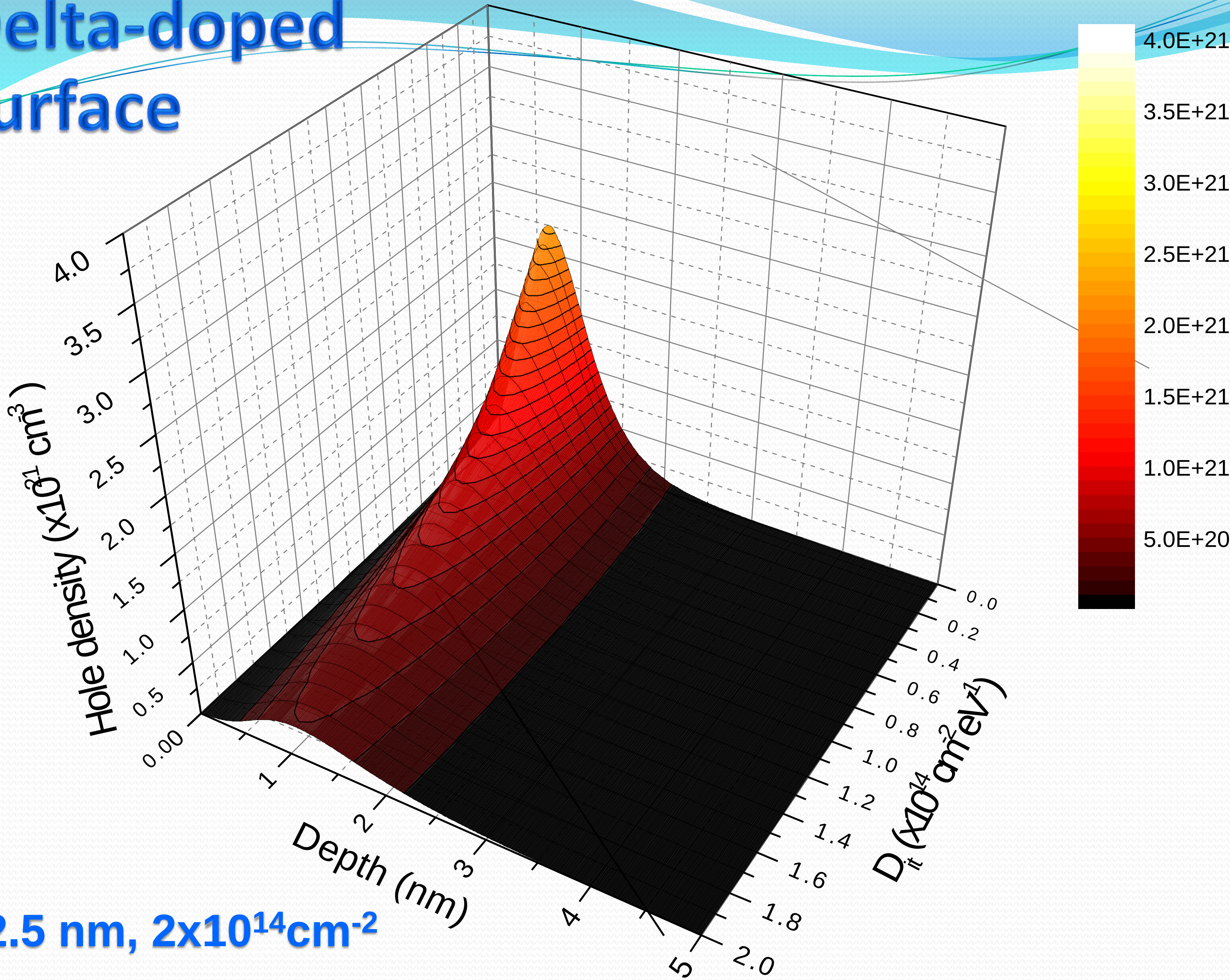

2.5 nm, $2 \times 10^{14} cm^{-2}$

Superlattice doped surface

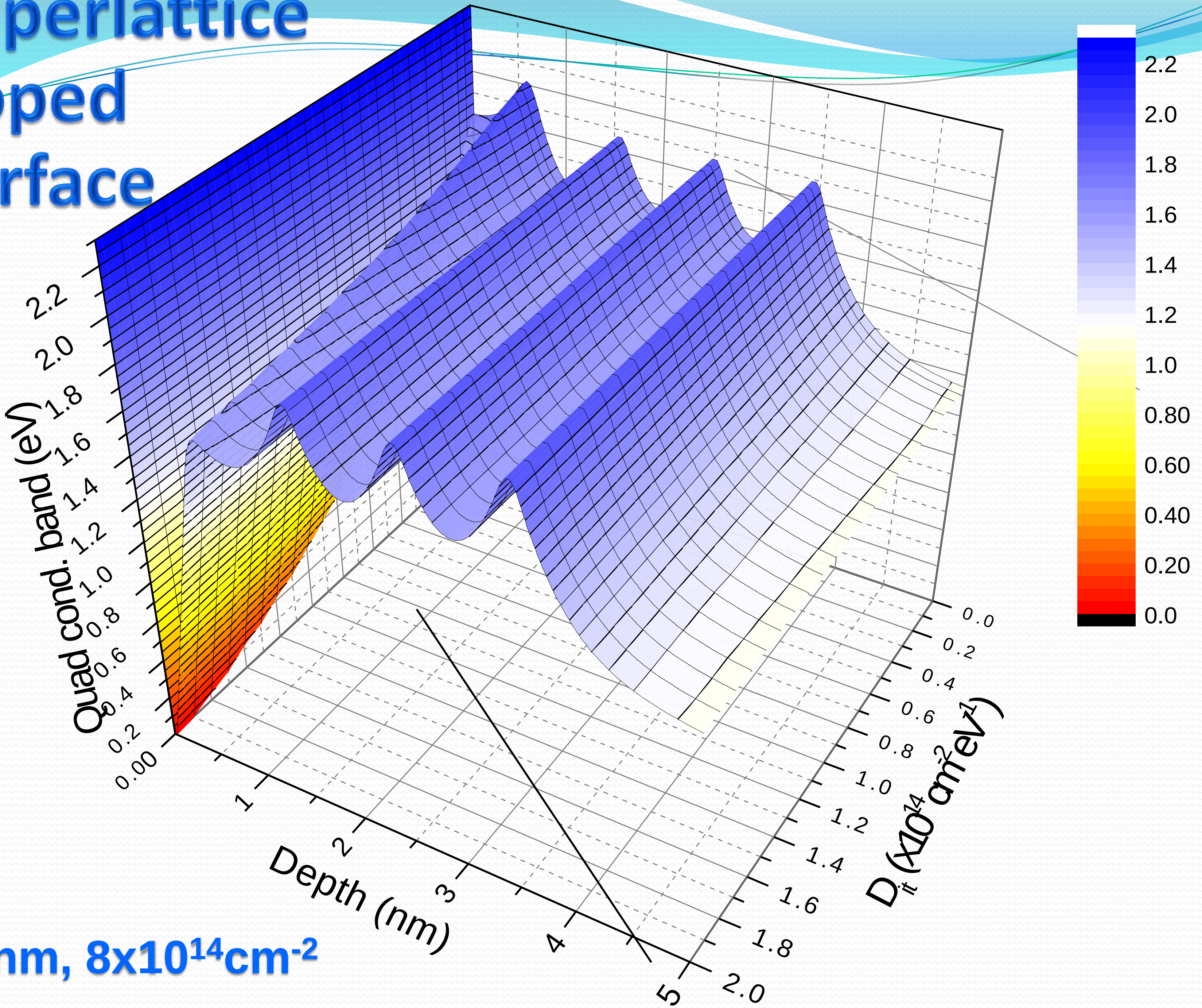

5 nm, 8x10^{14}cm^{-2}

Delta-doping Superlattice
Stable Far Ultraviolet CMOS Detectors

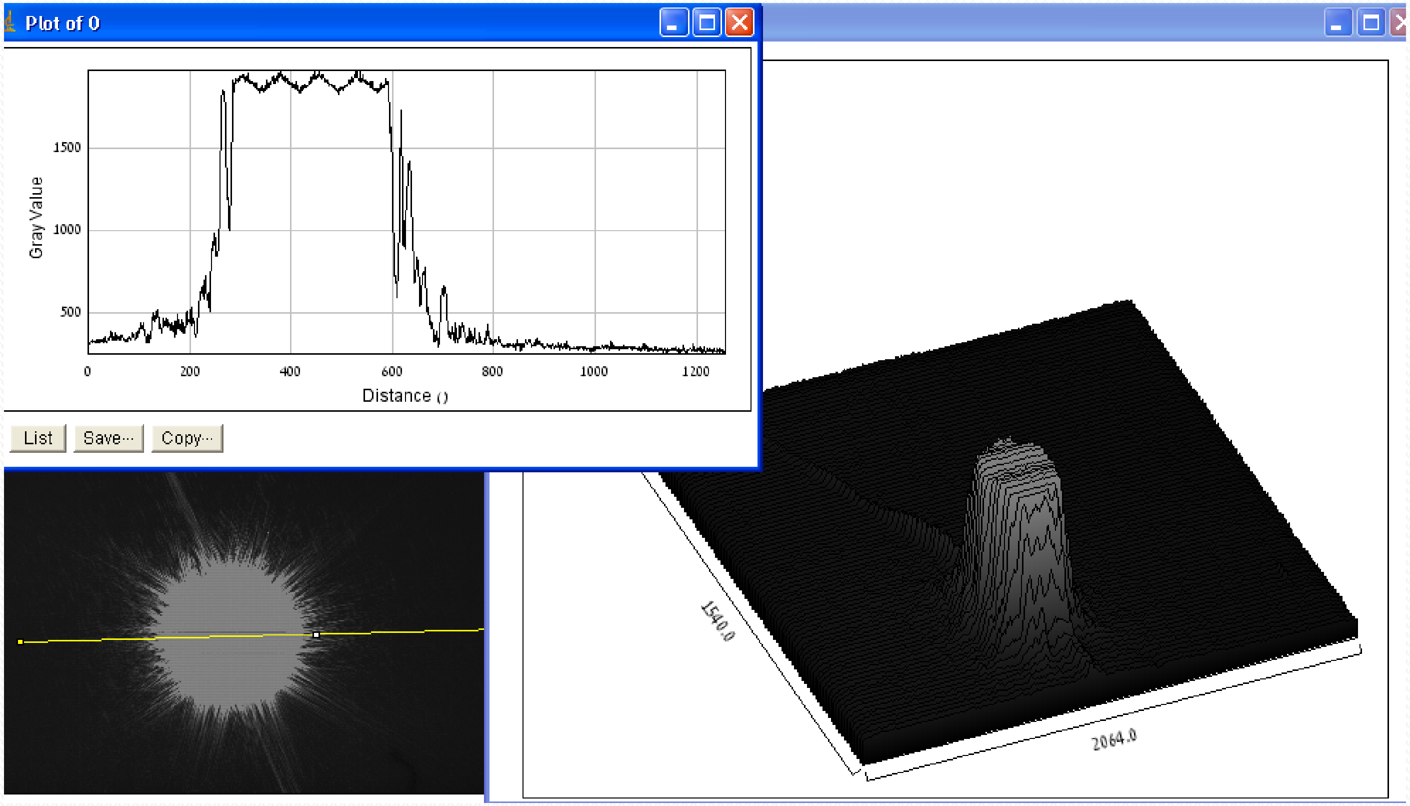

Superlattice passivation exhibits unique stability to FUV laser irradiation

- Pulsed excimer lasers: billions of pulses, > 3 kJ/cm^2
- Stability better than 1%
- No measurable persistence or hysteresis

Visible-blind, Superlattice-doped Silicon Detectors

- Molecular Beam Epitaxy
  - > 50% QE at 220 nm
  - Low dark current
  - High conductivity
  - Radiation tolerant

- Atomic Layer Deposition
  - Chemically passivated interface
  - Visible-blind AR coatings: < 1% QE at 330 nm

Current status

- We put in an ADR proposal to DOE for work on BaF_2/APDs
  - It was well-reviewed, but not funded
- We have some seed money to initiate work on the APD
  - Caltech/JPL/RMD collaboration, working toward an SBIR proposal
  - RMD has furnished six APD wafers to JPL for processing
    - Two stage development
      - Phase I: Extended UV response
      - Phase II: Integrate the interference filter
- If we can find some additional funds, will restart BaF_2 studies
  - Radiation hardness of modern samples
  - La (or other) doping to reduce the slow component fraction